Journal of Forensic and Legal Medicine 67 (2019) 37–48

Contents lists available at ScienceDirect

Journal of Forensic and Legal Medicine

journal homepage: www.elsevier.com/locate/yjflm

Research Paper

The microbiology, pH, and oxidation reduction potential of larval masses in decomposing carcasses on Oahu, Hawaii

Emily N. Junkins[a,1], Mark Speck[b], David O. Carter[a,*]

[a] Laboratory of Forensic Taphonomy, Forensic Sciences Unit, Division of Natural Sciences and Mathematics, Chaminade University of Honolulu, 3140 Waialae Avenue, Honolulu, HI, 96816, USA

[b] Division of Natural Sciences and Mathematics, Chaminade University of Honolulu, 3140 Waialae Avenue, Honolulu, HI, 96816, USA

ARTICLE INFO

Keywords:
Forensic taphonomy
Forensic microbiology
Postmortem microbiome
Decomposition
Postmortem interval
Oxidation reduction potential

ABSTRACT

Previous studies have begun to characterize the microbial community dynamics of the skin, soil, gut, and oral cavities of decomposing remains. One area that has yet to be explored in great detail is the microbiome of the fly larval mass, the community of immature flies that plays a significant role in decomposition. The current study aimed to characterize the microbiology and chemistry of larval masses established on pig (*Sus scrofa domesticus*) carcasses and to determine if these characteristics have potential as temporal evidence. Carcasses (n = 3) were decomposed on the soil surface of a tropical habitat on Oahu, Hawaii, USA and sampled over three days at 74 h, 80 h, 98 h, 104 h, 122 h, and 128 h (~85–142 Accumulated Degree Days) postmortem. Larval masses were analyzed via high-throughput 16S rRNA sequencing and *in situ* chemical measurements (pH, temperature, oxidation-reduction potential). A trend was observed that resulted in three distinct microbial communities (pre-98 h, 98 h, and post-98 h). The oxidation-reduction potential (Eh) of larval masses apparently regulated microbial community structure with the most negative Eh being associated with the least rich and diverse microbial communities. Overall, a significant interaction between time and taxa was observed, particularly with bacterial phyla Firmicutes and Proteobacteria. The current results provide new insight into the microbial community and chemical parameters of larval masses and indicate a temporal shift that could be further studied as a PMI estimator.

1. Introduction

Forensic microbiology is arguably one of the most rapidly developing fields in the forensic sciences.[1] This is because recent advances in sequencing technologies make it possible to identify prokaryote and eukaryote species that comprise microbial communities, calculate their relative abundance, and monitor shifts in their structure and function over time.[2,3] These analyses provide a fundamental understanding of postmortem microbial communities and their potential as physical evidence for criminal and medicolegal death investigation.[4] Traditionally forensic microbiology refers to the identification of microorganisms that cause death,[5,6] sometimes related to terrorist activity,[7] where microbiology is typically used as an adjunct to autopsies conducted in medical examiner and coroner offices. However, recent studies have identified much more forensic potential by analyzing microorganisms from a wide range of sites including soils,[8] water,[9] and many locations on decomposing remains including the mouth,[10] skin,[11–15] and nares.[16,17] These studies are investigating microbes as trace evidence[15] and estimators of postmortem interval (PMI).[3,12,13,16,18,19] Nevertheless, relatively little is understood about postmortem microbial communities and many locations on decomposing remains have yet to be investigated in great detail. One of these is the larval masses that play a significant role in the decomposition of remains.

To our knowledge, only one study has investigated the postmortem microbiome of the fly larval mass.[20] This microbial community[20] was dominated by phyla Proteobacteria and Firmicutes with some representatives from phyla Bacteroidetes and Fusobacteria, similar to previous studies in taxonomic composition.[2,3] Early stages of decomposition were primarily composed of both phyla Proteobacteria and Firmicutes in relatively even abundance with families Xanthomonadaceae (Proteobacteria) and Tissierellaceae (Firmicutes) being particularly abundant.[20] This study showed how the taxonomic structure of microbial communities associated with the skin, maggot mass and larvae change overtime as decomposition progresses. These trends are

* Corresponding author.
E-mail address: david.carter@chaminade.edu (D.O. Carter).
[1] Present Address: Department of Microbiology and Plant Biology, University of Oklahoma, 770 Van Vleet Oval, Norman, OK, 73019, USA.

https://doi.org/10.1016/j.jflm.2019.08.001
Received 28 January 2019; Received in revised form 2 July 2019; Accepted 8 August 2019
Available online 09 August 2019
1752-928X/ © 2019 Published by Elsevier Ltd.

of interest to forensic science as these types of shifts in community structure can be used to estimate postmortem interval, as demonstrated with forensic entomology.[21]

The current study aims to build upon the pioneering results of Weatherbee et al.[20] by providing further insight into the structure of the larval mass microbiome while incorporating *in situ* measurements of larval mass chemistry, including pH and oxidation-reduction potential (Eh). The advantages of characterizing postmortem chemistry is that it can be used to explain shifts observed in the microbial community while having the potential to serve as an additional form of physical evidence in its own right. The current project hypothesized that microbial community structure will change during decomposition as a carcass undergoes chemical changes, particularly changes in pH and Eh. The rationale for the current study stems from the efficacy of forensic entomology in estimating PMI. By conducting postmortem microbiology and chemistry, we can potentially decrease error in PMI estimation while providing chemical evidence in real time. Also, it is logical to hypothesize that the chemistry and microbiology of the larval mass follow predictable trends because the development of fly larvae follows predictable trends.

To investigate the microbiology and chemistry of larval masses, an experiment was conducted where three swine (*Sus scrofa domesticus*) carcasses were placed on the soil surface in a tropical savanna ecosystem on the island of Oahu, Hawaii. Samples to undergo Illumina rRNA gene sequencing were collected twice-daily from larval masses found on swine carcasses over the course of three days to correspond with peak maggot activity. Additionally, the chemistry of the sampling environment was studied in order to further characterize the environment associated with the larval mass microbiome.

2. Materials and methods

2.1. Decomposition site and swine carcasses

This research was conducted in June 2014. Three swine carcasses (*Sus scrofa domesticus*), each weighing approximately 25 kg, from Shinsato Farms in Kaneohe, Oahu, Hawaii, USA, were killed via electrocution under the Humane Slaughter Act (P.L. 85–765; 7 U S C. 1901) and placed in an outdoor decomposition site located in the Palalo Valley, Honolulu, Oahu, Hawaii within 1 h postmortem (21°17′27.4″N 157°48′17.7″W), as previously reported in Chun et al., 2015.[22] This particular decomposition site was on the side of a moderately steep hill in a tropical savanna ecosystem.[23] This site is approximately 285 feet above sea level with mean annual precipitation of approximately 700 mm, 70% of which occurs in the fall and winter seasons (October–March). The vegetation at the site is representative of a tropical savanna ecosystem on Oahu; it is rocky and dominated by guinea grass (*Megathyrsus maximus*) with night blooming cereus (*Hylocereus undatus*), aloe (*Aloe* spp.), and carrion plants (*Stapelia gigantia*). Few potential scavengers are present at the site; only the small Indian mongoose (*Herpestes javanicus*) have been observed in the region, as previously reported in Dibner et al.[11] The relative humidity (%) and temperature (°C) during the course of this survey were recorded using a datalogger (HOBO U23 Pro v2, Product #U23-001, Onset Corp., Cape Cod, MA, USA). Accumulated Degree Days (ADD) were calculated using 0 °C as the minimum developmental threshold.

2.2. Mass loss and Total Body Score

To determine the physical changes associated with carcass decomposition, carcasses were decomposed on top of weighing frames made from 3.8 cm diameter PVC pipe, galvanized steel chained-link fence, and 0.635 by 0.635 cm stainless steel mesh that were suspended and weighed using a hanging balance (Product No. H-110, American Weigh Scales Inc., Cumming, GA, USA), as described in Dibner et al.[11] (Fig. 1). Total Body Score (TBS) was calculated according to Megyesi et al.[24]

2.3. Sampling

Swabbing commenced when larval masses became visibly established throughout the carcass (~74 h postmortem). Swab samples were collected by inserting the swab (COPAN FLOQ Swabs, Lot# 6P0E00, Copan Diagnostics Inc, Murrieta, CA, USA) directly into the center of the larval mass. These samples were collected over the course of three days at 74 h, 80 h, 98 h, 104 h, 122 h, and 128 h postmortem, which corresponded to 1000 Hawaii Standard Time (HST) and 1600 HST each day and approximately 85 ADD to 142 ADD. Swabs were taken from a central region of the larval mass at a depth of approximately 2 cm. Throughout the course of decomposition, the position of the larval mass moved as the carcass was consumed, beginning in the oral cavity and migrating to the final sample taken from the abdominal cavity. Samples were collected from one carcass and five (n = 5) swabs were collected at each sampling event. Swabs were immediately placed in 15 ml sterile tubes (Product #89039–664, VWR International, West Chester, PA, USA), transported to the laboratory and stored at −20 °C until the survey was complete when swabs were shipped for 16S rRNA sequencing.

Temperature, pH, and Eh.

Chemical readings of the larval masses were obtained using a handheld, portable meter (Hach, Product #H170-G, Loveland, CO, USA) with sensors to measure temperature and pH (Hach, Product #PHW77-SS, Loveland, CO, USA) and Eh (Hach, Product #ORP110-GS, Loveland, CO, USA). Probes were inserted directly into the center of the larval mass.

2.4. 16S rRNA sequencing

Once the survey was complete, frozen (−20 °C) swabs were sent to Second Genome, Inc. in San Francisco, CA, for V4 16S rRNA sequencing. Genomic DNA was isolated using MoBio Bacteremia DNA Isolation Kit, as per vendor's protocol, and immediately stored at −20 °C. The resulting DNA ranged in concentration from 0 ng μl^{-1} to 0.55 ng ml^{-1}. All samples were quantified via the Qubit® Quant-iT dsDNA Broad-Range Kit (Invitrogen, Life Technologies, Grand Island, NY) to ensure that they met minimum concentration and mass of DNA. Bacterial 16S V4 rDNA region DNA was amplified using PCR primers 515F/806R and sequencing primers described by Caporaso et al.[25,26] designed against the surrounding conserved regions which are tailed with sequences to incorporate Illumina (San Diego, CA, USA) flow cell adapters and indexing barcodes. For each sample, amplified products were concentrated using a solid-phase reversible immobilization method for the purification of PCR products and quantified by electrophoresis using an Agilent 2100 Bioanalyzer. The pooled samples containing 30 16S rRNA gene V4-region amplified and barcoded samples were loaded into the MiSeq reagent cartridge, and then onto the instrument along with the flow cell. After cluster formation on the MiSeq instrument, the amplicons were sequenced for 250 cycles.

2.5. Sequence processing

Using QIIME and custom scripts, sequences were quality filtered and demultiplexed using exact matches to the supplied DNA barcodes. Resulting sequences were then searched against the Greengenes reference database of 16S rRNA gene sequences,[27,28] clustered at 97% by uclust (closed-reference OTU picking).[29] The longest sequence from each Operation Taxonomic Unit (OTU) was used as the representative sequence, and assigned taxonomic classification via mothur's Bayesian classifier,[30,31] trained against the Greengenes database clustered at 98%.[32] Taxa were filtered to those present in at least one of the samples, or to taxa significantly increased in their abundance in one category compared to the alternate categories. For the latter, ANOVA was used to calculate p-values. Additionally, q-values were calculated using the Benjamini-Hochberg procedure to correct p-values, controlling for false

Fig. 1. Decomposition of pig (*Sus scrofa domesticus*) carcasses in a tropical savanna habitat near Honolulu, Hawaii, USA in June 2014 over a period of 14 days. Carcasses were placed within 1 h postmortem (a) and progressed through the bloat (b), active decay (c), and advanced decay (d) stages of decomposition. Advanced decay was reached by 8 d postmortem.

discovery rates. It is important to note here that at the time of this study, Xanthomonadaceae was considered to be the family for *Ignatzschineria* spp., a commonly encountered bacterial genus observed in forensic decomposition. The SILVA database currently classifies this genus into family Wohlfhartiimonadaceae. The full classification remains to be determined. As such, this manuscript will retain the classification Xanthomonadaceae with the understanding that this designation is not officially recognized prokaryote nomenclature.

2.6. Summarization and sampling normalization

An ANOVA coupled with a Tukey post-hoc test was used to elucidate significant differences between genus richness and family abundance across multiple sample categories. Two approaches were used to account for uneven sequencing depth. 109,867 sequences were selected from each sample before calculating community-wide dissimilarity measures. This removed the bias due to sequencing depth that would otherwise affect Principal Coordinate Analysis (PCoA) plots and Adonis tests, among other analyses. Samples were normalized to 1 million counts, thus the relative abundance of each OTU represents the relative abundance in a sample per million sequences in that sample.

2.7. Sample-to-sample distance functions

All profiles were inter-compared in a pair-wise fashion to determine a dissimilarity score and store it in a distance/dissimilarity matrix. The distance functions were chosen to allow similar biological samples to produce small dissimilarity scores. The Weighted UniFrac dissimilarity uses the taxon abundance differences across samples but employed a pair-wise normalization by dividing the sum of differences by the sum of all abundances. The unweighted UniFrac metric, which considered only the presence or absence of taxa, was also used.

2.8. Ordination, clustering and classification methods

Two-dimensional ordinations and hierarchical clustering maps of the samples in the form of dendrograms were created to graphically summarize the inter-sample relationships. To create dendrograms, the samples from the distance matrix were clustered hierarchically using the average-neighbor method. Principal Coordinate Analysis (PCoA) is a method of two-dimensional ordination plotting that was used to visualize complex relationships between samples. PCoA used the dissimilarity values to position the points relative to each other.

2.9. Whole microbiome significance testing

Significant changes in the larval mass microbiome were determined by an Adonis test, a non-parametric, multivariate ANOVA using permutations (PERMANOVA). In this randomization/Monte Carlo permutation test, the samples were randomly reassigned to the various sample categories, and the mean normalized cross-category differences from each permutation were compared to the true cross-category differences. The fraction of permutations with greater distinction among categories (larger cross-category differences) than that observed with the non-permuted data was reported as the p-value for the Adonis test.

2.10. Univariate statistics

Univariate statistics were generated using Prism 7.0d for OS Mac (GraphPad Software Inc., La Jolla, CA). Because only some data sets were normal (Gaussian), both parametric and non-parametric statistics were generated. These included descriptive statistics, Spearman and Pearson correlations, Kruskall-Wallis tests, two-way ANOVAs with Tukey post-hoc comparisons, one-way ANOVA with Brown-Forsythe and Bartlett's tests, linear regressions, and ROC curves.

2.11. Multivariate statistics

Multivariate statistics were generated to explore the relationships between larval mass microbiology and chemistry. This was achieved using RStudio version 0.98.1102 (RStudio Inc.). Using *vegan* package, multivariate analyses were constructed using Bray-Curtis dissimilarity matrices with nonmetric multidimensional scaling (NMDS) in order to visualize differences between sampling communities. These multivariate statistics supplemented the initial QIIME processing.

3. Results

3.1. Environmental factors

During the course of this survey, the ambient temperature averaged at 26.8 °C with a range of 22.4 °C–33.9 °C. The relative humidity

Fig. 2. Several taphonomic changes were observed in a tropical savanna habitat near Honolulu, Hawaii, USA in June 2014 over a period of 14 days including marbling (a), abdominal rupture (b), skin slippage (c), and eventual bone exposure (d).

averaged at 68.7% with a range of 42.2%–93.7%. The carcasses were exposed to peak heat between the late morning (1000 HST) to late afternoon (1600 HST) during which carcasses were not shaded. Additionally, carcasses experienced one brief shower between 100 h (113 ADD) and 120 h (142 ADD) postmortem from which no maggots appeared disturbed or washed away.

3.2. Gross decomposition

All carcasses appeared fresh with no signs of bloating when initially placed at the decomposition facility (Fig. 1a). Only slight lividity was observed on one carcass in this early postmortem period (2 h postmortem). At 8 h postmortem, carcasses were bloated, and decomposition fluids were being released from the orifices of one carcass (Fig. 1b). At 26 h (~29 ADD) postmortem, all carcasses were bloated with reddish purple discoloration in the neck and abdomen and observable maggot eggs in the oral cavities. Marbling was observed in the chest of one of the carcasses (Fig. 2a) and one carcass exhibited a herniated intestine by this time (Fig. 2b).

The other two carcasses presented the same herniation by 32 h postmortem so that all carcasses were associated with exposed, bloated intestinal organs (Fig. 2b). By this time the skin of all three carcasses was darker, transitioning from reddish purple to a dark purple/green discoloration, and small larval masses were present. Peak larval activity was initially observed at 74 h (~85 ADD) postmortem, when the bloated abdomens were beginning to collapse (Fig. 2c). As decomposition progressed the exposed intestines and other tissues appeared to desiccate as the larval masses moved throughout the remains. By 104 h (~113 ADD) postmortem, the carcasses were relatively dry with exposed bones and dried skin covered in dark brown/black grease (Fig. 2d). Larval activity began to decrease from this time until 128 h (~142 ADD) postmortem, when chemical measurements ceased due to the lack of an adequate larval mass for the probes.

3.3. Mass loss and Total Body Score (TBS)

Carcass mass loss followed a pattern typical of outdoor decomposition[11,33] with an initial period of little mass loss (< 10%) from 0 h to 32 h (~39 ADD) postmortem (Fig. 3a). Mass loss was more rapid after this time, with ~20% mass loss by 56 h (~60 ADD) postmortem and ~80% mass loss by 176 h (~200 ADD) postmortem. Measurements were taken until 384 h (435 ADD) postmortem, by which time mass loss remained constant at ~80% (Fig. 3a). Much like mass loss, TBS followed a similar pattern in which the initial period of little decomposition climbed rapidly as decomposition progressed only to plateau later in decomposition (Fig. 3b). In fact, a significant ($p < 0.001$, $R^2 = 0.951$) positive correlation was observed between mass loss and TBS (Fig. 3c).

3.4. Larval mass temperature, pH, and Eh

Larval masses observed on the carcasses were sampled from 74 h–128 h (~85 ADD – 142 ADD) postmortem as they migrated from the oral cavity along the length of the carcass with the final mass observed in the abdominal cavity. Larval masses were warm habitats with mean temperature ranging from 31.0 °C ± 1.2 °C–39.1 °C ± 1.2 °C (Fig. 3d). The temperature of the larval masses was relatively constant at ~35 °C (Fig. 3d) and generally greater than mean ambient temperature of 26.8 °C. Larval mass pH was generally neutral with most values between 6.5 and 7.5. Larval mass pH increased from 6.4 ± 0.5 to 7.4 ± 0.2 between 74 h and 104 h postmortem (Fig. 3e). A more acidic pH (6.7 ± 0.1) was observed at 122 h (~142 ADD) postmortem, however, pH was again alkaline (7.7 ± 0.1) by 128 h postmortem. Lastly, Eh indicated a reducing environment with little to no available oxygen as it ranged from −79 mV ± 31 mV to −283 mV ± 11 mV to (Fig. 3f). Oxidation reduction potential was more positive over time, which may indicate an increased availability of oxygen as decomposition progressed. The goal of the study was to investigate microbial community shifts within the larval mass over the course of

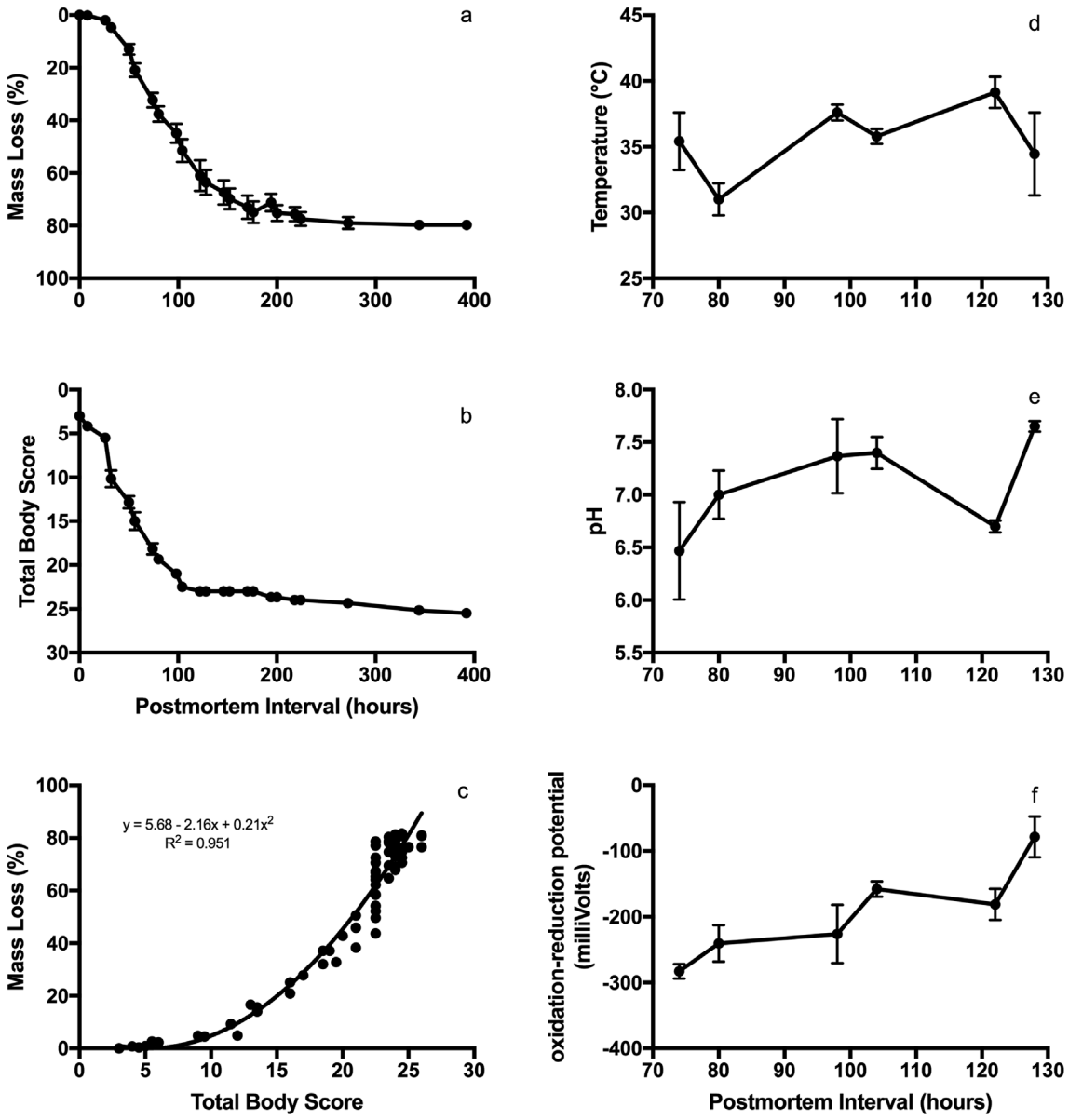

Fig. 3. Decomposition and chemical metrics associated with of pig (*Sus scrofa domesticus*) carcasses in a tropical savanna habitat near Honolulu, Hawaii, USA in June 2014 over a period of 14 days. Carcass mass loss (a) and Total Body Score (b) were significantly ($p < 0.001$) positively correlated (c). Fly larval mass temperature (d), pH (e), and oxidation-reduction potential (f), were measured between 74 and 128 h postmortem. Error bars represent standard error where n = 3 for each pig carcass.

decomposition relative and the chemical changes within the larval mass over time. No insect species, adult or larvae, were identified for the purposes of this study. However, as a field observation, both adult flesh flies (Diptera: Sarcophagidae) and blow flies (Diptera: Calliphoridae) were present at the decomposition site.

3.5. Microbiome structure

Nine prokaryote phyla were detected (7 Bacteria, 2 Archaea). However, larval mass microbiomes were consistently dominated by three bacterial phyla: Actinobacteria, Firmicutes, and Proteobacteria while the other phyla represented ≤1% of the whole microbiome (Fig. 4). Consistently abundant bacterial families included Clostridiacaeae (Firmicutes), Enterococcaceae (Firmicutes), Lactobacillaceae (Firmicutes), Mogibacteriaceae (Firmicutes), Peptostreptococcaceae (Firmicutes), and Xanthomonadaceae (Proteobacteria) (Fig. 4). A similar representation of taxa was observed at the genus level, as *Clostridium* (Firmicutes), *Enterococcus* (Firmicutes), *Ignatzschineria* (Proteobacteria), *Lactobacillus* (Firmicutes), and *Peptostreptococcus* (Firmicutes) were the most abundant genera.

Overall, microbial diversity was relatively low, similar to the observation of Weatherbee et al.,[20] and diversity decreased until 98 h (~113 ADD) postmortem, after which time an increase was observed (Fig. 5). Corresponding shifts in microbiome structure were observed as the abundance of six phyla (Actinobacteria, Bacteroidetes, Euryarchaeota, Firmicutes, Proteobacteria, Tenericutes) also shifted significantly ($p < 0.001$) over time. Most remarkable were the shifts observed over three sampling periods (80 h–98 h – 104 h, ~85 ADD – 120 ADD) when phylum Proteobacteria become most abundant (77% ± 2%) and the abundance of Firmicutes was 23% ± 2%; the abundance of Firmicutes ranged from 88% to 98% at all other times. This shift was driven by an increase in the abundance of *Ignatzschineria* sp., a bacterial species regularly associated with blow flies and flesh flies.[34,35] These observations, along with results from the Adonis test

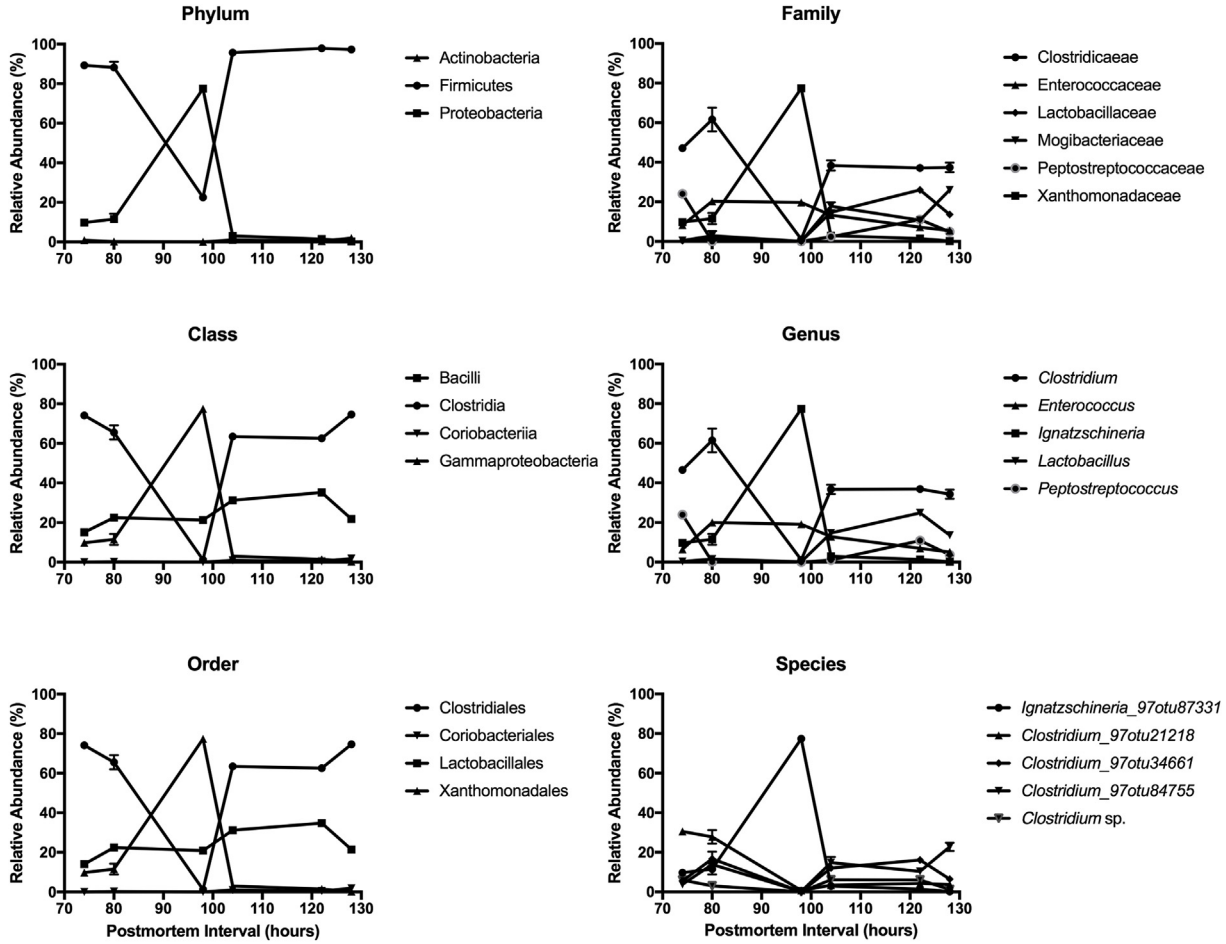

Fig. 4. Relative abundance of bacteria collected from larval masses established in pig (*Sus scrofa domesticus*) carcasses in a tropical savanna habitat near Honolulu, Hawaii, USA in June 2014 from 74 h–128 h postmortem. Taxa shown regularly represented ≥2% of the whole microbiome. Error bars represent standard error where n = 5 for each replicate swab.

($p < 0.001$), prompted the organization and analysis of the microbiome as three potentially distinct groups, Pre-98 h, 98 h, and Post-98 h (Pre-113 ADD, 113 ADD, Post-113 ADD).

The Pre-98 h microbiomes were associated with a relatively low temperature, neutral pH, and low Eh (Table 1). During these two sampling times (74 h, 80 h; ~85 ADD - 113 ADD) the microbial community was dominated by genera *Clostridium*, *Enterococcus*, *Ignatzschineria*, and *Peptostreptococcus*. In contrast, the microbiome at 98 h (113 ADD) postmortem was associated with greater pH, temperature, and Eh (Table 1). The 98 h community was also the least rich (Fig. 5), as only two dominant genera were observed: *Ignatzschineria* and *Enterococcus*. Subsequently, the Post-98 h (Post-113 ADD) microbiomes were associated with similarly high temperature and pH with a greater Eh (Table 1). These microbial communities were dominated by bacterial genera *Clostridium*, *Enterococcus*, and *Peptostreptococcus* along with two new dominant genera: *Lactobacillus* and *Gallicola*. The structure of these microbiomes was most strongly associated with Eh ($p < 0.001$) that could be observed by distinct clustering (Fig. 6), with insignificant associations with temperature ($p = 0.324$) and pH ($p = 0.313$).

Oxidation reduction potential had a significant effect on the abundance of several taxa, particularly those from phylum Firmicutes (Fig. 7). Some of these taxa (e.g. *Clostridium, Ignatzschineria*) demonstrated a clear preference for more strongly reducing habitats while other taxa (e.g. *Mogibacterium*, Peptostreptococcaceae) were more abundant at a lesser Eh. In fact, Eh influenced the structure of the whole microbiome, as more reducing environments were consistently associated with less diverse communities (Fig. 8).

4. Discussion

The current data show that carcasses decomposed rapidly; approximately 80% of carcass mass was decomposed by seven days postmortem. This rapid decomposition was associated with fly larval masses readily visible from 74 h–128 h (~85 ADD – 142 ADD) postmortem. Significant changes in the microbiology and chemistry of these larval masses were observed over time. Generally, the larval mass was a reducing environment of high temperature and neutral pH that supported a microbiome dominated by bacterial phyla Firmicutes and Proteobacteria. Microbial communities tended to be dominated by Firmicutes, but a significant shift in the abundance of Proteobacteria was observed at 98 h (~113 ADD) postmortem. Larval mass chemistry played a significant role in microbial community structure, as it was significantly driven by oxidation reduction potential. Furthermore, a more negative oxidation reduction potential was consistently associated with less microbial diversity. These observations lead to the conclusion that a fly larval mass is a dynamic ephemeral habitat that supports rapid shifts in microbial community structure, which are driven by the availability of oxygen and nutrients. Furthermore, these observations complement two recent studies into the microbiology[20] and chemistry[22] of larval masses and may have implications for entomology-based estimates of PMI.

Weatherbee et al.[20] investigated larval mass microbiomes associated with pig carcasses in West Lafayette, Indiana, USA and also observed larval mass microbiomes dominated by Firmicutes and Proteobacteria with an inverse relationship in the abundance of these two phyla (e.g.

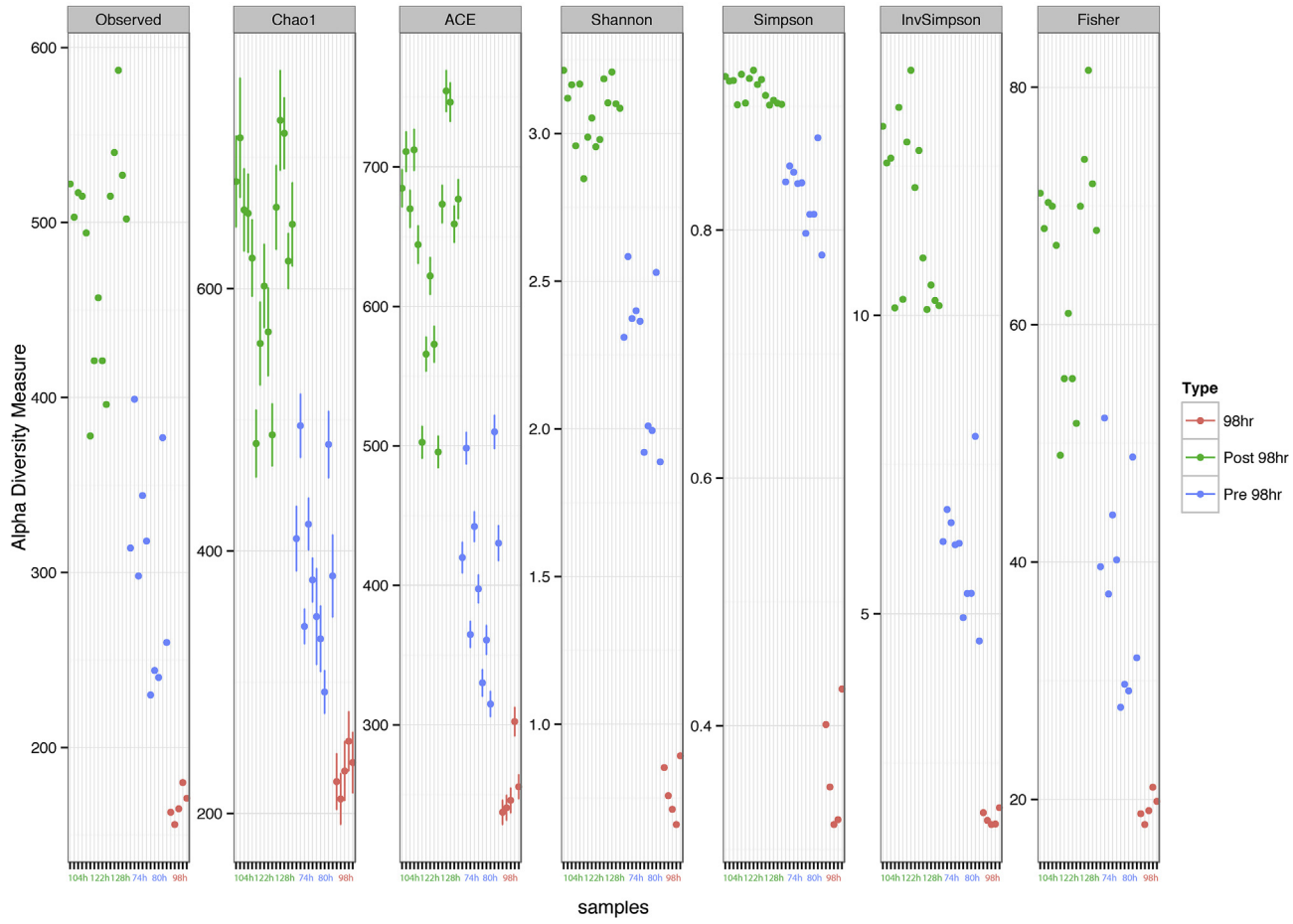

Fig. 5. Alpha diversity of microbiomes collected from larval masses established in pig (*Sus scrofa domesticus*) carcasses in a tropical savanna habitat near Honolulu, Hawaii, USA in June 2014 from 74 h–128 h postmortem. Postmortem microbiomes were grouped into three PMIs: Pre-98 h, 98 h, and Post-98 h based on differing levels of diversity indicating that 98 h postmortem was associated with the lowest overall microbial diversity. Alpha diversity measures include Chao1, Abundance Based Coverage Estimator (ACE) along with the Shannon, Simpson, Inverse Simpson, and Fisher indices.

Pechal et al., 2014). Furthermore, the microbiomes were dominated by similar bacterial families, including Xanthomonadaceae and Clostridiaceae. The abundance of these bacteria may be related to insect abundance, as they[20] observed that an increase in the abundance of the blow fly *Phormia regina* corresponded to an increase in Xanthomonadaceae. This type of interaction might explain the abundance of genus *Ignatzschineria* in the current study. Relatively little is known about this taxon but it is known to have associations with blow flies and flesh flies,[34,35] both of which were observed in the current study. *Ignatzschineria* may rely on these insects for transportation between resources, possibly via a symbiotic or phoretic relationship like those observed between nematodes and insects.[36] *Ignatzschineria* may then, once established, be responsible for volatile organic compounds (VOCs) that attract subsequent insects to the remains. Insects are well known to respond to VOCs released by microorganisms.[37] Jordan and Tomberlin[38] point out that different fly species may demonstrate preference for different microbial communities; a better understanding of these relationships might enhance entomology-based estimates of postmortem interval.

Another recent experiment,[22] conducted at the same site as the current study, also observed a fly larval mass as a reducing habitat of high temperature and neutral pH. Although Chun et al.[22] used culture-based techniques to characterize the larval mass microbial community, they successfully cultured several genera collected from larval masses, many of which were also observed in the current study including *Bacillus, Enterococcus*, and *Ignatzschineria*. These observations represent important progress for forensic microbiology because they demonstrate some level of similarity in larval mass microbiomes across climates,

Table 1
Microbiology of larval masses established in pig (*Sus scrofa* domesticus) carcasses in a tropical savanna habitat near Honolulu, Hawaii, USA in June 2014 from 74 h–128 h postmortem. Dominant genera regularly represented > 2% of the whole microbiome. Oxidation reduction potential (Eh) was measured in milliVolts (mV) and all data are presented with ± standard error where n = 3.

Postmortem interval	pH	Eh (mV)	Temperature (°C)	Dominant genera
74 – 98 h	6.4 ± 0.5–7.0 ± 0.2	−240 ± 28 mV – −283 ± 11 mV	31 ± 1 °C – 35 ± 2 °C	*Clostridium Enterococcus Ignatzschineria Peptostreptococcus*
98 h	7.4 ± 0.4	−226 ± 45 mV	38 ± 1 °C	*Enterococcus Ignatzschineria*
98 – 128 h	6.7 ± 0.1–7.7 ± 0.1	−79 ± 31 mV – −181 ± 24 mV	34 ± 3 °C – 39 ± 1 °C	*Clostridium Enterococcus Gallicola, Lactobacillus Peptostreptococcus*

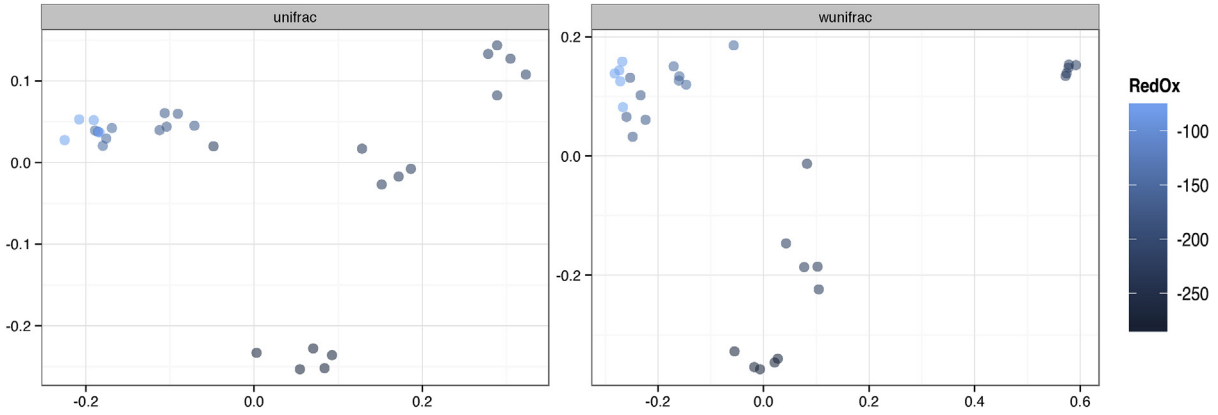

Fig. 6. Unweighted (presence/absence: UniFrac) and Weighted (relative abundance: wUniFrac) beta diversity measures using Bray-Curtis distances of larval mass of microbiomes collected from larval masses established in pig (*Sus scrofa domesticus*) carcasses in a tropical savanna habitat near Honolulu, Hawaii, USA in June 2014 from 74 h–128 h postmortem. Blue coloration gradient indicates oxidation-reduction potential associated with each sample. (For interpretation of the references to color in this figure legend, the reader is referred to the Web version of this article.)

geography, years, and microbial identification techniques. This similarity probably indicates that a fly larval mass is a specialized habitat that can only be inhabited by certain microorganisms and may represent an example of convergence. Convergence is an ecological process where two separate microbial communities become similar to one another over time, typically following the introduction of nutrients or contaminants. Convergence of microbial communities collected from mouse and human remains across seasons and soil types has been observed where the microbiome from one carcass species was used to accurately estimate the PMI of a different carcass species.[3] Establishing the level of similarity between postmortem microbiomes across variables is an important step forward for forensic microbiology because it may allow for the use of nonhuman models to develop forensic tools.[39,40]

In the current study, the structure of microbiomes at all times other than 98 h postmortem was dominated by phylum Firmicutes. Genera *Clostridium*, *Enterococcus*, and *Peptostreptococcus* each represented 20% of the whole microbiome during at least one sampling period. Genus *Clostridium* consistently represented at least 35% of the whole microbiome. These taxa have been observed in association with several other recent studies[2,18,41–44] and the prevalence of *Clostridium* spp. in the current study may represent an example of the Postmortem Clostridium Effect.[41] *Clostridium* is an anaerobic taxon that can proliferate during decomposition because it can tolerate highly reducing conditions (Fig. 7); microbial activity is so great that all available oxygen is consumed rapidly. Several species of *Clostridium* have been associated with decomposing remains,[21,41,42,45] so this genus is probably a major contributor to several postmortem processes including putrefaction[41] and scavenger activity.[46]

Oxidation reduction potential is commonly used to indicate the oxygen status of a habitat and infer the most probable products of microbial metabolism.[47] The oxidation reduction potential of the larval masses in the current study (approximately -300 mV – -100 mV) indicate a habitat suitable for anaerobes (e.g. *Clostridium*) that is likely associated with the reduction of sulfate and carbon dioxide to hydrogen sulfide and methane, respectively.[47] These VOCs are regularly associated with decomposing remains and can play a significant role in the activity of insects and scavengers.[48] In addition, hydrogen sulfide is a gas associated with putrefaction and bloating that can react with haemoglobin to result in some of the color changes observed during decomposition.[49,50] The metabolic products will change as oxygen is introduced to the system and the structure of the microbiome changes; Fig. 7 shows that different microbial taxa proliferate at different Eh values. For example, a habitat associated with an Eh of approximately +220 mV would indicate the reduction of nitrate to form ammonium, which is a compound regularly associated with decomposing remains.[51–53] The current results indicate that the structure of the larval mass microbiome observed in the current study was significantly regulated by the availability of oxygen and nutrients, while pH and temperature apparently played a lesser role in microbiome structure.

Another intriguing observation is the apparent influence of rainfall on the pH and Eh of the decomposition environment and microbial community. Rainfall can significantly alter the microbiology and chemistry of habitats by providing access to soluble carbon and nutrients and facilitating microbial motility.[54] This essentially provides pulses of resources to microbial communities, which results in a flush of microbial activity. The current study was associated with brief rainfall event (< 2 mm) on day 5 (~142 ADD) postmortem. This event was followed by significant ($p < 0.05$) increases in larval mass pH and Eh between 120 h and 130 h postmortem (Fig. 3). These data may be indicative of denitrification, which is a key step in the nitrogen cycle whereby anaerobic microbial metabolism reduces nitrate to nitrogen gas. Although nitrogenous compounds were not measured in the current study, the pH (7.6), Eh (−79 mV), and temperature (34 °C) observed at 128 h postmortem are within the optimal range for denitrification.[55] These data also demonstrate the importance of the environment in decomposition processes, particularly the availability of moisture. The observed rainfall was unremarkable when considered in context of the weather regularly observed at the decomposition site; it is not uncommon for the site to receive multiple rainfall events that each provide ≥2 mm of precipitation during a study. Yet, the relatively little rainfall observed in the current study apparently contributed to a significant change in pH, Eh, and microbial community structure.

From a forensic perspective, understanding the relationships between microbes and insects has significant potential for forensic entomology and forensic microbiology.[56] Postmortem bacteria, particularly genera *Proteus*, *Providencia*, and *Ignatzschineria* release VOCs that can attract and trigger oviposition of several forensically important flies.[37,48] Subsequently, microbial communities also contribute to the growth and development of insects. For example, Crooks et al.[57] observed that the presence of bacterial species *Escherichia coli* and *Staphylococcus aureus* affected the growth rates of blow fly species *Calliphora vomitoria* and *Calliphora vicina*. Additionally, insects can transport microbes to and from decomposing remains. This type of relationship (phoresy) is well established between flies and microbes and may play a critical role in the structure and function of postmortem microbiomes. *Rhabditis stammeri*, for example, is a nematode that is transported by insects, particularly the burying beetle *Nicrophorus vespilloides*.[58] This relationship contributes directly to the structure of postmortem microbiomes. A number of recent studies have observed postmortem

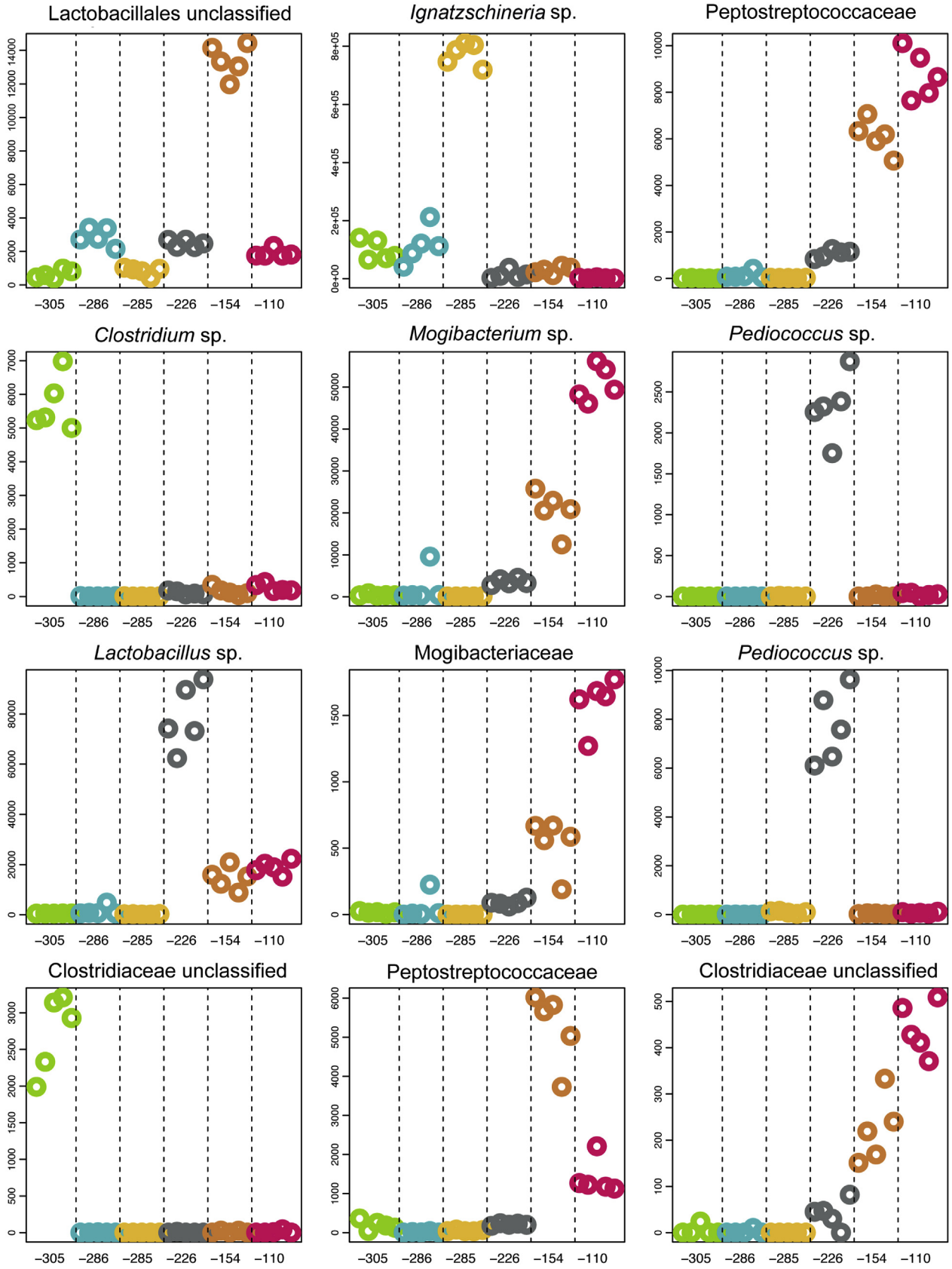

Fig. 7. Redox potentials associated with selected bacterial taxa collected from larval masses established in pig (*Sus scrofa domesticus*) carcasses in a tropical savanna habitat near Honolulu, Hawaii, USA in June 2014 from 74 h–128 h postmortem. Oxidation-reduction potential directly affected the relative abundance of specific taxa where colors correspond to oxidation reduction potential (milliVolts) along the x-axis and the y-axis indicates OTU abundance. (For interpretation of the references to color in this figure legend, the reader is referred to the Web version of this article.)

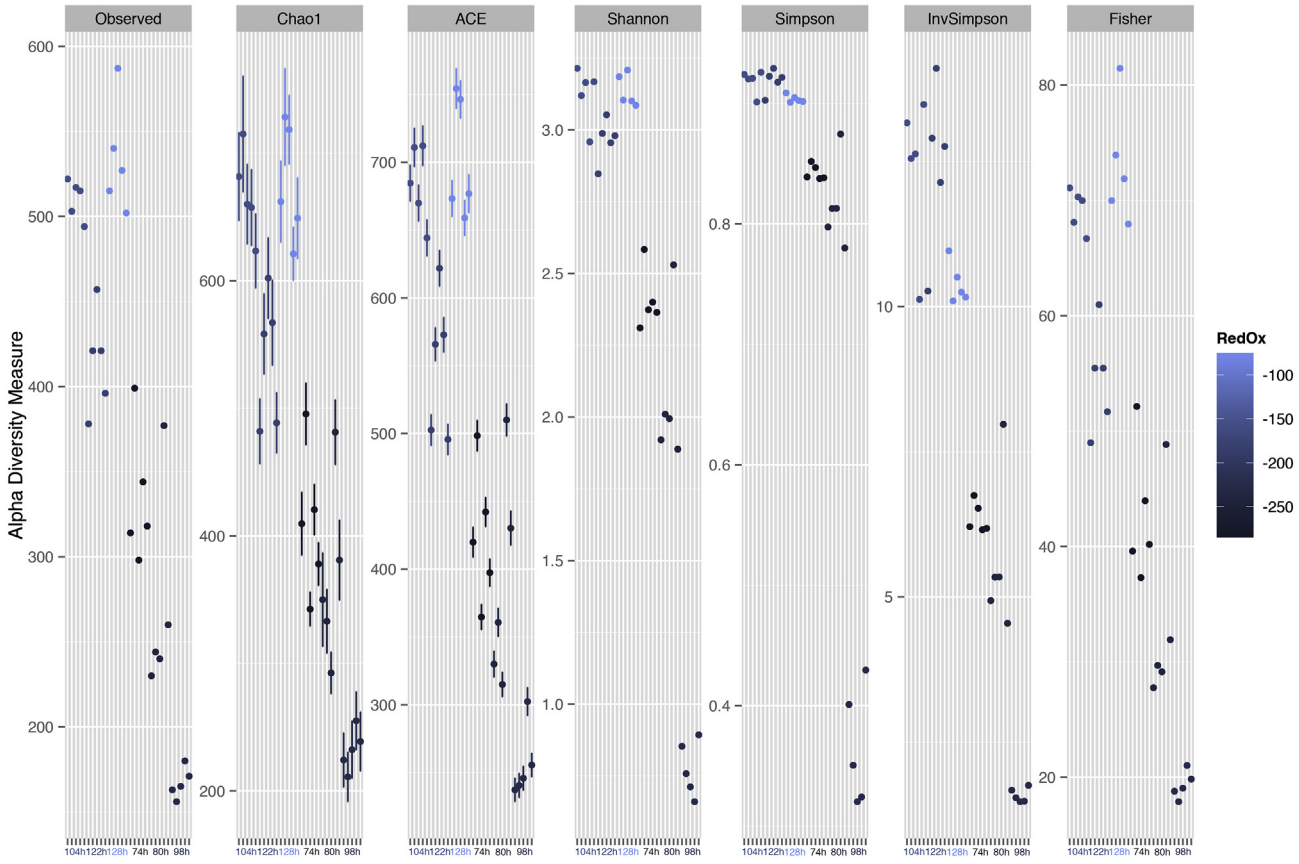

Fig. 8. Alpha diversity of microbiomes collected from larval masses established in pig (*Sus scrofa domesticus*) carcasses in a tropical savanna habitat near Honolulu, Hawaii, USA in June 2014 from 74 h–128 h postmortem. Postmortem microbiomes were grouped by oxidation reduction potential (Redox; milliVolts) indicating that 98 h postmortem was associated with the greatest reducing environment and the lowest microbial diversity. Alpha diversity measures include Chao1, Abundance Based Coverage Estimator (ACE) along with the Shannon, Simpson, Inverse Simpson, and Fisher indices.

bacteria, such as *Ignatzschineria* and *Wohlfahrtiimonas*, in close association with forensically relevant insects.[20,22] Indeed, much of what is known about *Ignatzschineria* is due to research into the interactions between this bacterium and flies (Diptera: Sarcophagidae).[34] Thus, a robust understanding of insect-microbe interactions is particularly important for estimating PMI, as many of these estimates are based on the rapid colonization and healthy development of insects.

Another interesting observation was the significant positive correlation between carcass mass loss and TBS. Decomposition can be measured in several ways; Megyesi et al.[24] developed TBS as a means to use macroscopic postmortem changes as a metric for decomposition and PMI. The current results are insightful because they demonstrate that visual postmortem change can be significantly correlated to mass loss, a direct measurement of decomposition. This is an important observation because it might facilitate the use of the recent equation proposed by Vass,[59] which requires an estimate of soft tissue mass loss.[60] However, this relationship requires more detailed study, as TBS can overestimate mass loss in the early postmortem period and underestimate mass loss in the extended postmortem period.[61] It would be helpful to investigate this relationship in other parts of the world especially where seasonal differences in temperature and precipitation are significant.

Our understanding of postmortem microbiology is advancing rapidly. Several recent studies have demonstrated that a myriad of microorganisms, including archaea,[62] bacteria,[63] nematodes,[64] mites,[65] amoeba,[66] and enchytraeids[67] have significant potential as probative physical evidence. The current study contributes to forensic microbiology by providing new insight into the microbial ecology of the larval mass. Specifically, larval masses were warm, reducing, pH neutral environments associated with significant changes in microbiology and chemistry over time. This habitat selected for a microbiome dominated by phyla Firmicutes and Proteobacteria, particularly genera *Clostridium*, *Enterococcus*, *Gallicola*, *Ignatzschineria*, *Lactobacillus*, and *Peptostreptococcus*. These observations may eventually lead to a more robust forensic microbiology, including an improved understanding of microbial-based estimates of PMI.[12,13,16,18,68] Eventually, employing postmortem microbiology and chemistry together with forensic entomology can potentially increase accuracy in PMI estimation.

Declarations of interest

None.

Conflicts of interest

The author(s) declare(s) that there is no conflict of interest.

Funding

This work was supported by the Air Force Research Laboratory and Clarkson Aerospace Minority Leaders Program [MSC/PA-2018-0239] and the National Institutes of Health – Building Research Infrastructure and Capacity Program [P789097-876].

Acknowledgments

We kindly thank L. Chan, D. Morton, and J. Oka from Second Genome, Inc. for assistance with sample processing and data analysis.

We are very thankful to H. Harakuni for assistance with data analysis. We also thank A. Orimoto and K. Thompson for assistance with sample collection at Chaminade University of Honolulu Decomposition Facility.

References

1. Carter DO, Tomberlin JK, Benbow ME, Metcalf JL, eds. *Forensic Microbiology*. Chichester, UK: Wiley-Blackwell; 2017.
2. Pechal JL, Schmidt CJ, Jordan HR, Benbow ME. A large-scale survey of the post-mortem human microbiome, and its potential to provide insight into the living health condition. *Sci Rep.* 2018;8:5724. https://doi.org/10.1038/s41598-018-23989-w.
3. Metcalf JL, Xu ZZ, Weiss S, et al. Microbial community assembly and metabolic function during mammalian corpse decomposition. *Science.* 2016;351(80):158–162.
4. Burcham ZM, Jordan HR. History, current, and future use of microorganisms as physical evidence. In: Carter DO, Tomberlin JK, Benbow ME, Metcalf JL, eds. *Forensic Microbiology*. Chichester, UK: John Wiley & Sons, Ltd.; 2017:25–55.
5. Richey DG, Goehring C. Studies on bacteriemias in the agonal period. *J Media Res.* 1918;38:421–447.
6. Ridgway EJ, Subramanian BM, Raza M. Clinical microbiology and virology in the context of the autopsy. In: Carter DO, Tomberlin JK, Benbow ME, Metcalf JL, eds. *Forensic Microbiology*. Chichester, UK: John Wiley & Sons, Ltd.; 2017:146–191.
7. Fujinami Y, Hosokawa-Muto J, Mizuno N. Evaluation of tools for environmental sampling of *Bacillus anthracis* spores. *Forensic Sci Int.* 2015;257:376–378.
8. Finley SJ, Pechal JL, Benbow ME, Robertson BK, Javan GT. Microbial signatures of cadaver gravesoil during decomposition. *Microb Ecol.* 2016;71:524–529.
9. Benbow ME, Pechal JL, Lang JM, Erb R, Wallace JR. The potential of high-throughput metagenomic sequencing of aquatic bacterial communities to estimate the post-mortem submersion interval. *J Forensic Sci.* 2015;60:1500–1510.
10. Hyde ER, Haarmann DP, Lynne AM, Bucheli SR, Petrosino JF. The living dead: bacterial community structure of a cadaver at the onset and end of the bloat stage of decomposition. *PLoS One.* 2013;8. https://doi.org/10.1371/journal.pone.0077733.
11. Dibner H, Mancga Valdez C, Carter DO. An experiment to characterize the decomposer community associated with carcasses (*Sus scrofa domesticus*) on Oahu. *Hawaii.J. Forensic Sci.* 2019https://doi.org/10.1111/1556-4029.14009.
12. Metcalf JL, Parfrey LW, Gonzalez A, et al. A microbial clock provides an accurate estimate of the postmortem interval in a mouse model system. *Elife.* 2013:e01104https://doi.org/10.7554/eLife/01104.
13. Pechal JL, Crippen TL, Benbow ME, Tarone AM, Dowd S, Tomberlin JK. The potential use of bacterial community succession in forensics as described by high throughput metagenomic sequencing. *Int J Leg Med.* 2014;128:193–205.
14. Iancu L, Dean DE, Purcarea C. Temperature influence on prevailing necrophagous Diptera and bacterial taxa with forensic implications for postmortem interval estimation: a review. *J Med Entomol.* 2018. https://doi.org/10.1093/jme/tjy136.
15. Kodama WA, Xu ZZ, Metcalf JL, et al. Trace evidence potential in postmortem skin microbiomes: from death scene to morgue. *J Forensic Sci.* 2019;64:791–798.
16. Johnson HR, Trinidad DD, Guzman S, et al. A maching learning approach for using the postmortem skin microbiome to estimate the postmortem interval. *PLoS One.* 2016;11. https://doi.org/10.1371/journal.pone.0167370.
17. Pechal JL, Schmidt CJ, Jordan HR, Benbow ME. Frozen: thawing and its effect on the postmortem microbiome in two pediatric cases. *J Forensic Sci.* 2017;62:1399–1405.
18. Hauther KA, Cobaugh KL, Jantz LM, Sparer TE, DeBruyn JM. Estimating time since death from postmortem human gut microbial communities. *J Forensic Sci.* 2015;60:1234–1240.
19. Damann FE, Williams DE, Layton AC. Potential use of bacterial community succession in decaying human bone for estimating postmortem interval. *J Forensic Sci.* 2015;60:844–850.
20. Weatherbee CR, Pechal JL, Benbow ME. The dynamic maggot mass microbiome. *Ann Entomol Soc Am.* 2017;110(1):45–53.
21. Iancu L, Carter DO, Junkins EN, Purcarea C. Using bacterial and necrophagous insect dynamics for post-mortem interval estimation during cold season: novel case study in Romania. *Forensic Sci Int.* 2015;254:106–117.
22. Chun LP, Miguel MJ, Junkins EN, Forbes SL, Carter DO. An initial investigation into the ecology of culturable aerobic postmortem bacteria. *Sci Justice.* 2015;55:394–401.
23. Peel MC, Finlayson BL, McMahon TA. Updated world map of the Köppen-Geiger climate classification. *Hydrol Earth Syst Sci.* 2007;11:1633–1644.
24. Megyesi MS, Nawrocki SP, Haskell NH. Using accumulated degree-days to estimate the postmortem interval from decomposed human remains. *J Forensic Sci.* 2005;50:618–626.
25. Caporaso JG, Lauber CL, Walters WA, et al. Ultra-high-throughput microbial community analysis on the Illumina HiSeq and MiSeq platforms. *ISME J.* 2012;6:1621–1624.
26. Caporaso JG, Lauber CL, Walters WA, et al. Global patterns of 16S rRNA diversity at a depth of millions of sequences per samples. *Proc Natl Acad Sci USA.* 2011;108:4516–4522.
27. DeSantis TZ, Hugenholtz P, Larsen N, et al. Greengenes, a chimera-checked 16S rRNA gene database and workbench compatible with ARB. *Appl Environ Microbiol.* 2006;72:5069–5072.
28. Caporaso JG, Bittinger K, Bushman FD, Desantis TZ, Andersen GL, Knight R. PyNAST: a flexible tool for aligning sequences to a template alignment. *Bioinformatics.* 2010;26:266–267.
29. Edgar RC. Search and clustering orders of magnitude faster than BLAST. *Bioinformatics.* 2010;26:2460–2461.
30. Wang Q, Garrity GM, Tiedje JM, Cole JR. Naïve Bayesian classifier for rapid assignment of rRNA sequences into the new bacterial taxonomy. *Appl Environ Microbiol.* 2007;73:5261–5267.
31. Schloss PD, Westcott SL, Ryabin T, et al. Introducing mothur: open-source, platform-independent, community-supported software for describing and comparing microbial communities. *Appl Environ Microbiol.* 2009;75:7537–7541.
32. McDonald D, Price MN, Goodrich J, et al. An improved Greengenes taxonomy with explicit ranks for ecological and evolutionary analyses of bacteria and archaea. *ISME J.* 2012;6:610–618.
33. Carter DO, Yellowlees D, Tibbett M. Cadaver decomposition in terrestrial ecosystems. *Naturwissenschaften.* 2007;94:12–24.
34. Gupta AK, Dharne MS, Rangrez AY, et al. *Ignatzschineria indica* sp. nov. and *Ignatzschineria ureiclastica sp.* nov., isolated from adult flesh flies (Diptera: Sarcophagidae). *Int J Syst Evol Microbiol.* 2011;61:1360–1369.
35. Tóth EM, Borsodi AK, Euzéby JP, Tindall BJ, Márialigeti K. Proposal to replace the illegitimate genus name *Schineria* Tóth et al. 2001 with genus name *Ignatzschineria* gen. nov. and to replace the illegitimate combination *Schineria larvae* Tóth et al. 2001 with *Ignatzschineria larvae* comb. *Int J Syst Evol Microbiol.* 2007;57:179–180.
36. Timper P, Davies KG. Biotic interactions. In: Gaugler R, Bilgrami AL, eds. *Nematode Behaviour*. Wallingford, UK: CABI Publishing; 2004:277–306.
37. Ma Q, Fonseca A, Liu W, et al. *Proteus mirabilis* interkingdom swarming signals attract blow flies. *ISME J.* 2012;6:1356–1366.
38. Jordan HR, Tomberlin JK. Abiotic and biotic factors regulating inter-kingdom engagement between insects and microbe activity on vertebrate remains. *Insects.* 2017;8. https://doi.org/10.3390/insects8020054.
39. Metcalf JL. Estimating the postmortem interval using microbes: knowledge gaps and hurdles. *Forensic Sci Int Genet.* 2019;38:211–218.
40. Matuszewski S, Hall MJR, Moreau G, Schoenly KG, Tarone AM, Villet MH. Pigs vs people: the use of pigs as analogues for humans in forensic entomology and taphonomy research. *Int J Leg Med.* 2019https://doi.org/10.1007/s00414-019-02074-5.
41. Javan GT, Finley SJ, Miller J, Wilkinson JE. Cadaver thanatomicrobiome signatures: the ubiquitous nature of *Clostridium* species in human decomposition. *Front Microbiol.* 2017;8. https://doi.org/10.3389/fmicb.2017.02096.
42. DeBruyn JM, Hauther KA. Postmortem succession of gut microbial communities in deceased human subjects. *PeerJ.* 2017;5. https://doi.org/10.7717/peerj.3437.
43. Guo J, Fu X, Liao H, et al. Potential use of bacterial community succession for estimating post-mortem interval as revealed by high-throughput sequencing. *Sci Rep.* 2016;6 101038/srep.24197.
44. Heimesaat MM, Boelke S, Fischer A, et al. Comprehensive postmortem analyses of intestinal microbiota changes and bacterial translocation in human flora associated mice. *PLoS One.* 2012;7. https://doi.org/10.1371/journal.pone.0040758.
45. Hyde ER, Haarmann DP, Petrosino JF, Lynne AM, Bucheli SR. Initial insight into bacterial succession during human decomposition. *Int J Leg Med.* 2015;129:661–671.
46. Meng X, Lu S, Yang J, et al. Metataxonomics reveal vultures as a reservoir for *Clostridium perfringens*. *Emerg Microb Infect.* 2017;6:e9.
47. Voroney RP. The soil habitat. In: Paul EA, ed. *Soil Microbiology, Ecology, and Biochemistry*. third ed. Burlington, MA, USA: Academic Press; 2007:25–49.
48. Verheggen F, Perrault KA, Megido RC, et al. The odor of death: an overview of current knowledge on characterization and applications. *Bioscience.* 2017;67:600–613.
49. Gill-King H. Chemical and ultrastructural aspects of decomposition. In: Haglund WD, Sorg MH, eds. *Forensic Taphonomy: The Postmortem Fate of Human Remains*. Boca Raton, FL, USA: CRC Press; 1997:93–108.
50. Clark MA, Worrell MB, Pless JE. Postmortem changes in soft tissues. In: Haglund WD, Sorg MH, eds. *Forensic Taphonomy: The Postmortem Fate of Human Remains*. Boca Raton, FL, USA: CRC Press; 1997:151–164.
51. Anderson B, Meyer J, Carter DO. Dynamics of ninhydrin-reactive nitrogen and ph in gravesoil during the extended postmortem interval. *J Forensic Sci.* 2013;58:1348–1352.
52. Meyer J, Anderson B, Carter DO. Seasonal variation of carcass decomposition and gravesoil chemistry in a cold (Dfa) climate. *J Forensic Sci.* 2013;58(5):1175–1182.
53. Szelecz I, Koenig I, Seppey CVW, Le Bayon R-C, Mitchell EAD. Soil chemistry changes beneath decomposing cadavers over a one-year period. *Forensic Sci Int.* 2018;286:155–165.
54. Cruz-Martinez K, Rosling A, Zhang Y, Song M, Andersen GL, Banfield JF. Effect of rainfall-induced soil geochemistry dynamics on grassland soil microbial communities. *Appl Environ Microbiol.* 2012;78:7587–7595.
55. Robertson GP, Groffman PM. Nitrogen transformations. In: Paul EA, ed. *Soil Microbiology, Ecology, and Biochemistry*. third ed. Burlington, MA, USA: Academic Press; 2007:341–364.
56. Tomberlin JK, Crippen TL, Tarone AM, et al. A review of bacterial interactions with blow flies (Diptera: Calliphoridae) of medical, veterinary, and forensic importance. *Ann Entomol Soc Am.* 2017;110:19–36.
57. Crooks ER, Bulling MT, Barnes KM. Microbial effects on the development of forensically important blow fly species. *Forensic Sci Int.* 2016;266:185–190.
58. Richter S. Phoretic association between dauerjuveniles of *Rhabditis stammeri* (Rhabditidae) and life history stages of the burying beetle *Nicrophorus vespilloides* (Coleoptera: silphidae). *Nematologica.* 1993;39:346–355.
59. Vass AA. The elusive universal postmortem interval formula. *Forensic Sci Int.* 2011;204:34–40.
60. Maile AE, Inoue CG, Barksdale LE, Carter DO. Toward a universal equation to estimate postmortem interval. *Forensic Sci Int.* 2017;272:150–153.
61. Ribéreau-Gayon A, Rando C, Morgan RM, Carter DO. The suitability of visual taphonomic methods for digital photographs: an experimental approach with pig carcasses in a tropical climate. *Sci Justice.* 2017;58:167–176.
62. Kwon MJ, Yun S-T, Ham B, Lee J-H, Oh J-S, Jheong W-W. Impacts of leachates from livestock carcass burial and manure heap sites on groundwater geochemistry and

microbial community structure. *PLoS One.* 2017;12. https://doi.org/10.1371/journal.pone.0182579.
63. Lauber CL, Metcalf JL, Keepers K, Ackermann G, Carter DO, Knight R. Vertebrate decomposition is accelerated by soil microbes. *Appl Environ Microbiol.* 2014;80(16):4920–4929.
64. Szelecz I, Sorge F, Seppey CVW, et al. Effects of decomposing cadavers on soil nematode communities over a one-year period. *Soil Biol Biochem.* 2016;103:405–416.
65. Szelecz I, Lösch S, Seppey CVW, et al. Comparative analysis of bones, mites, soil chemistry, nematodes and soil micro-eukaryotes from a suspected homicide to estimate the post-mortem interval. *Sci Rep.* 2018;8:25. https://doi.org/10.1038/s41598-017-18179-z.
66. Wanner M, Betker E, Shimano S, Krawczynski R. Are soil testate amoebae and diatoms useful for forensics? *Forensic Sci Int.* 2018;289:223–231.
67. Schlaghamerský J, Krawczynski R. Does carcass decomposition affect soil-dwelling enchytraeids? *Soil Org.* 2015;87:91–100.
68. Belk A, Xu ZZ, Carter DO, et al. Microbiome data accurately predicts the postmortem interval using random forest regression models. *Genes.* 2018;9. https://doi.org/10.3390/genes9020104.